Properties of individual nanoparticles

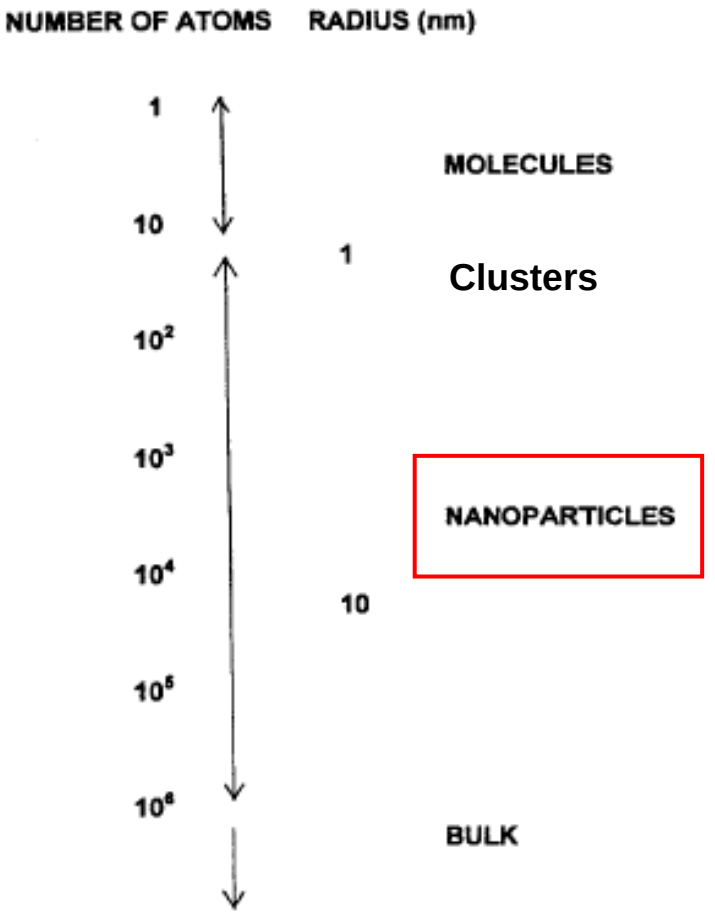

Particle nature of photons

Einstein's proposal:

$E = h\nu \Rightarrow P = h/\lambda$

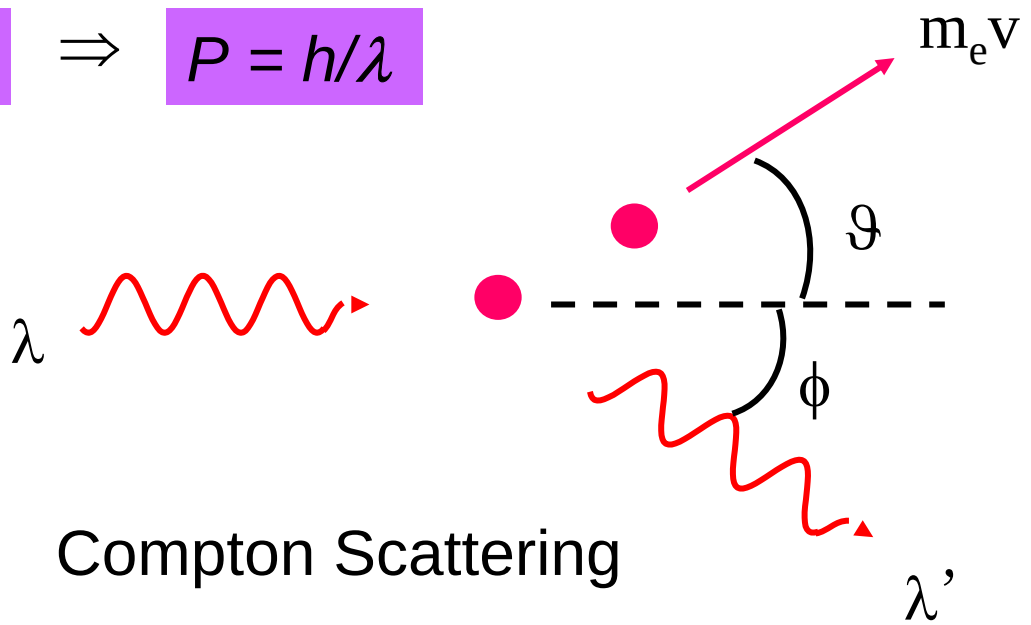

Compton Scattering

Wave nature of electrons

de Broglie's proposal:

$\lambda = h/P \Rightarrow \nu = h/E$

For electrons:

$\lambda\,(nm) = 1.22/E^{1/2}(eV)$

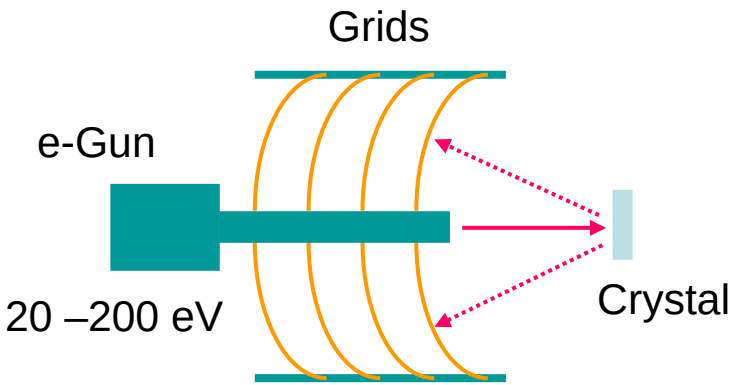

LEED

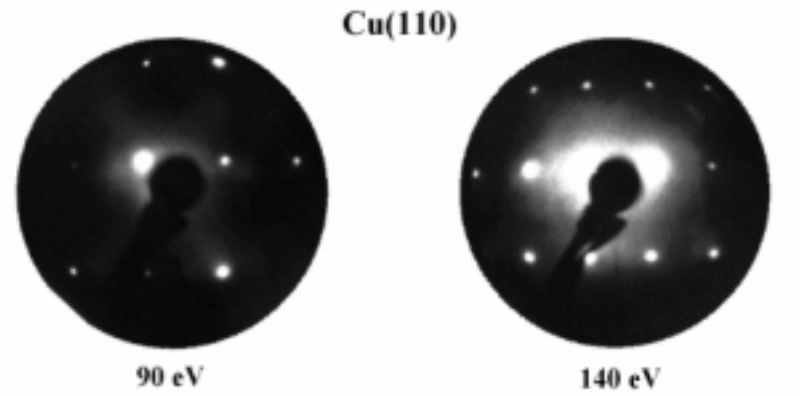

Fundamentals of quantum mechanics

1. Quantization

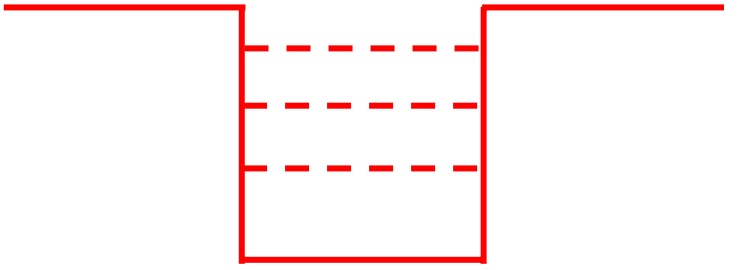

2. Tunneling

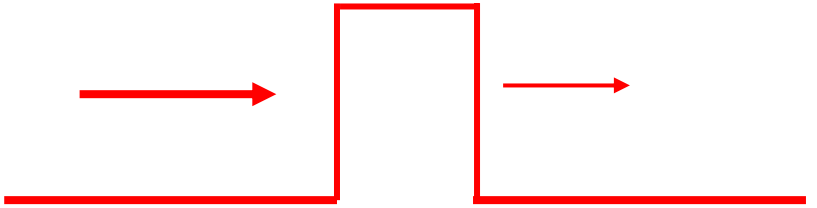

3. Statistics

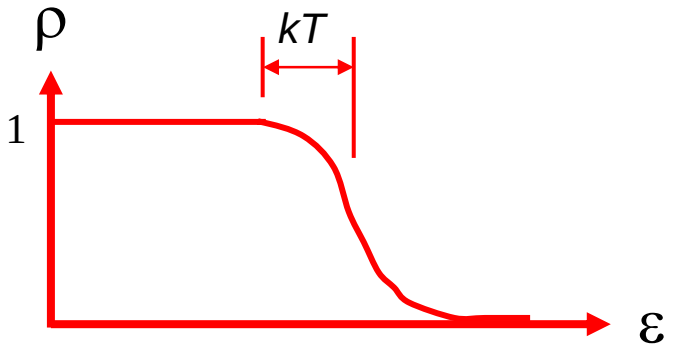

Critical Length scale

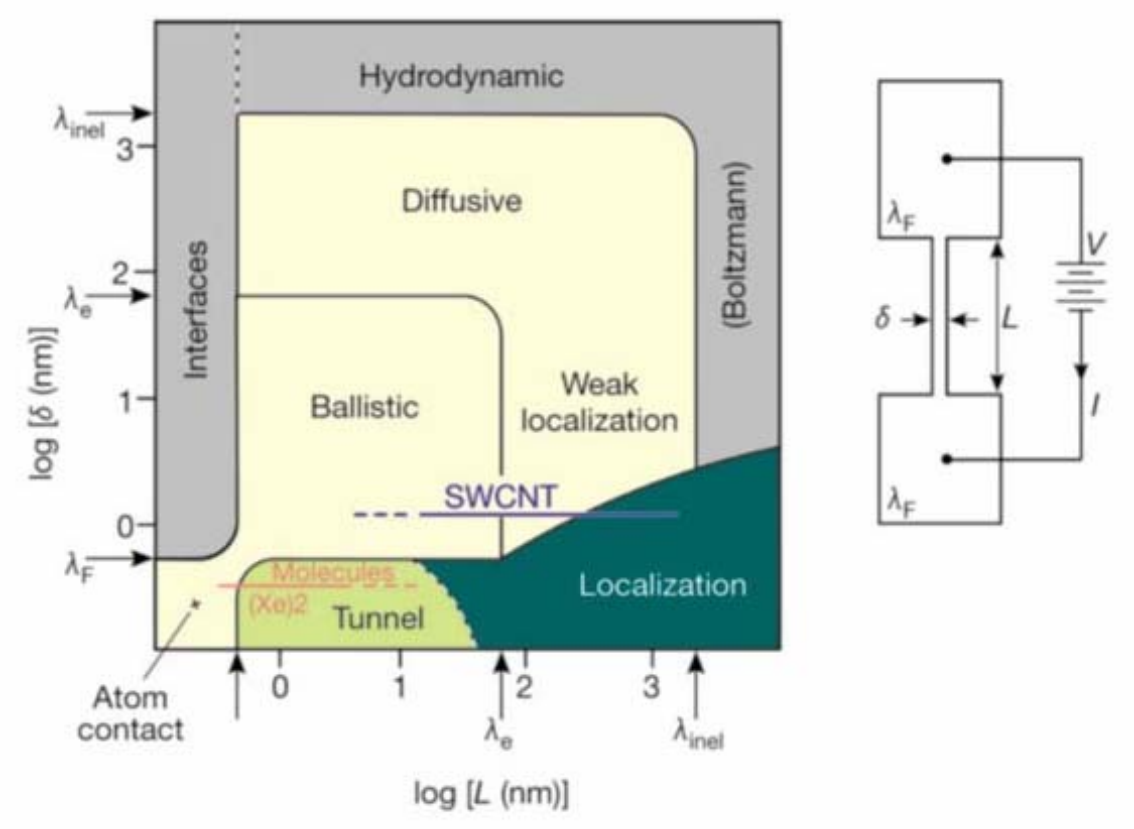

C. Joachim *et al., Nature* 408, 541 (2000).

One dimensional size effect

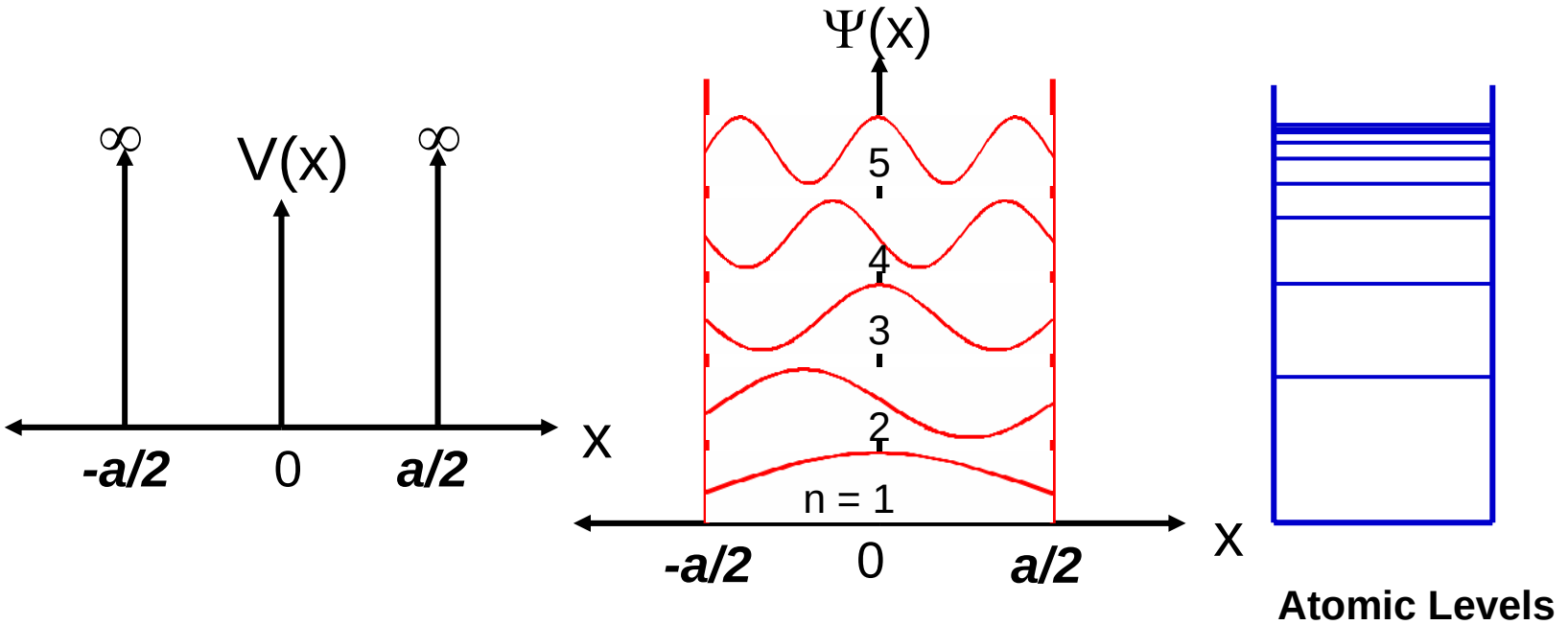

$$\Psi(x) = \begin{cases} \sin(n\pi x/a), & n \text{ even} \\ \cos(n\pi x/a), & n \text{ odd} \end{cases}$$

$$E = n^2\pi^2\hbar^2/2ma^2,\ n = 1,2,3\ldots$$

Size effect

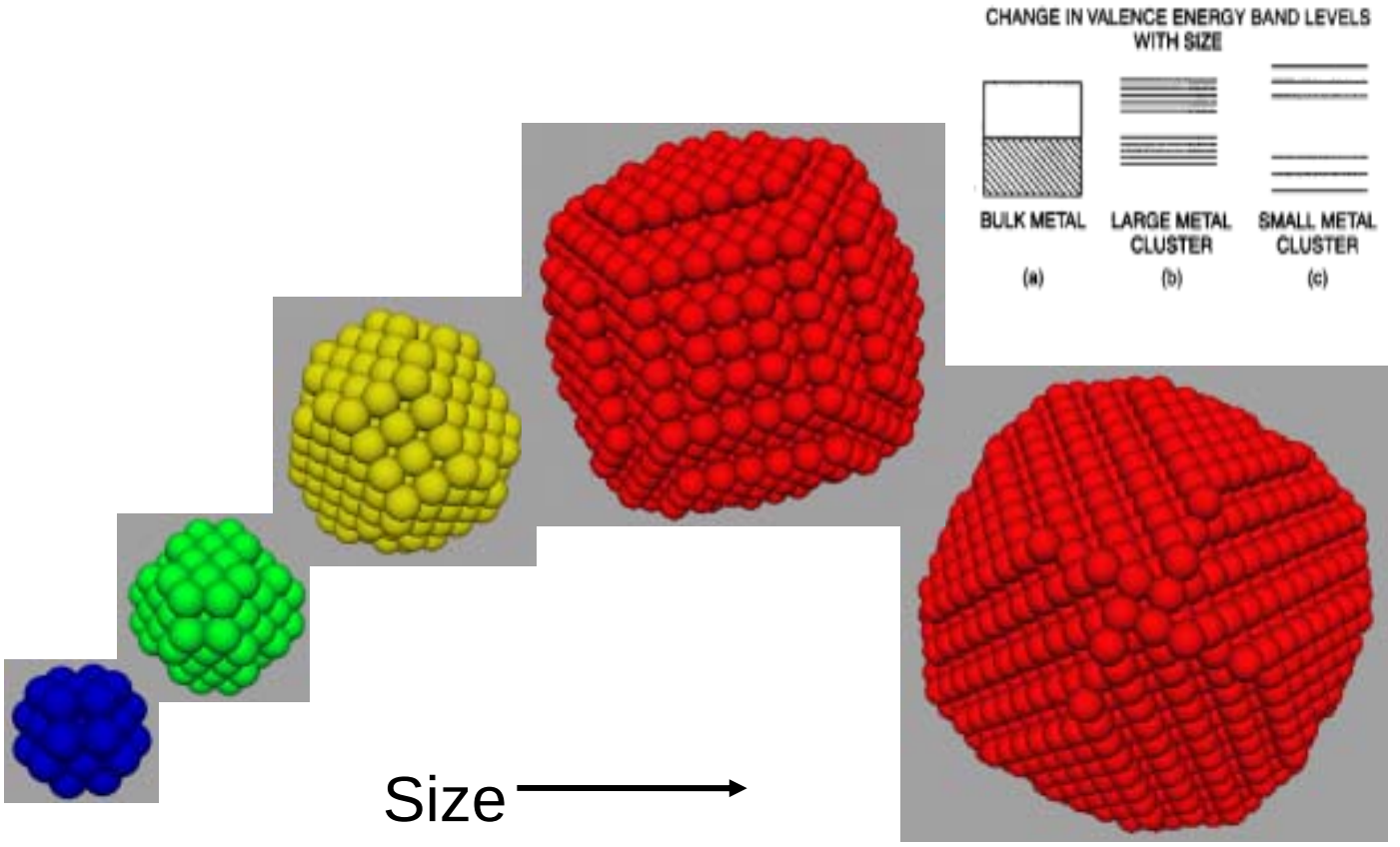
CHANGE IN VALENCE ENERGY BAND LEVELS WITH SIZE
BULK METAL
LARGE METAL CLUSTER
SMALL METAL CLUSTER
(a)
(b)
(c)
Size

Ratio of surface atoms

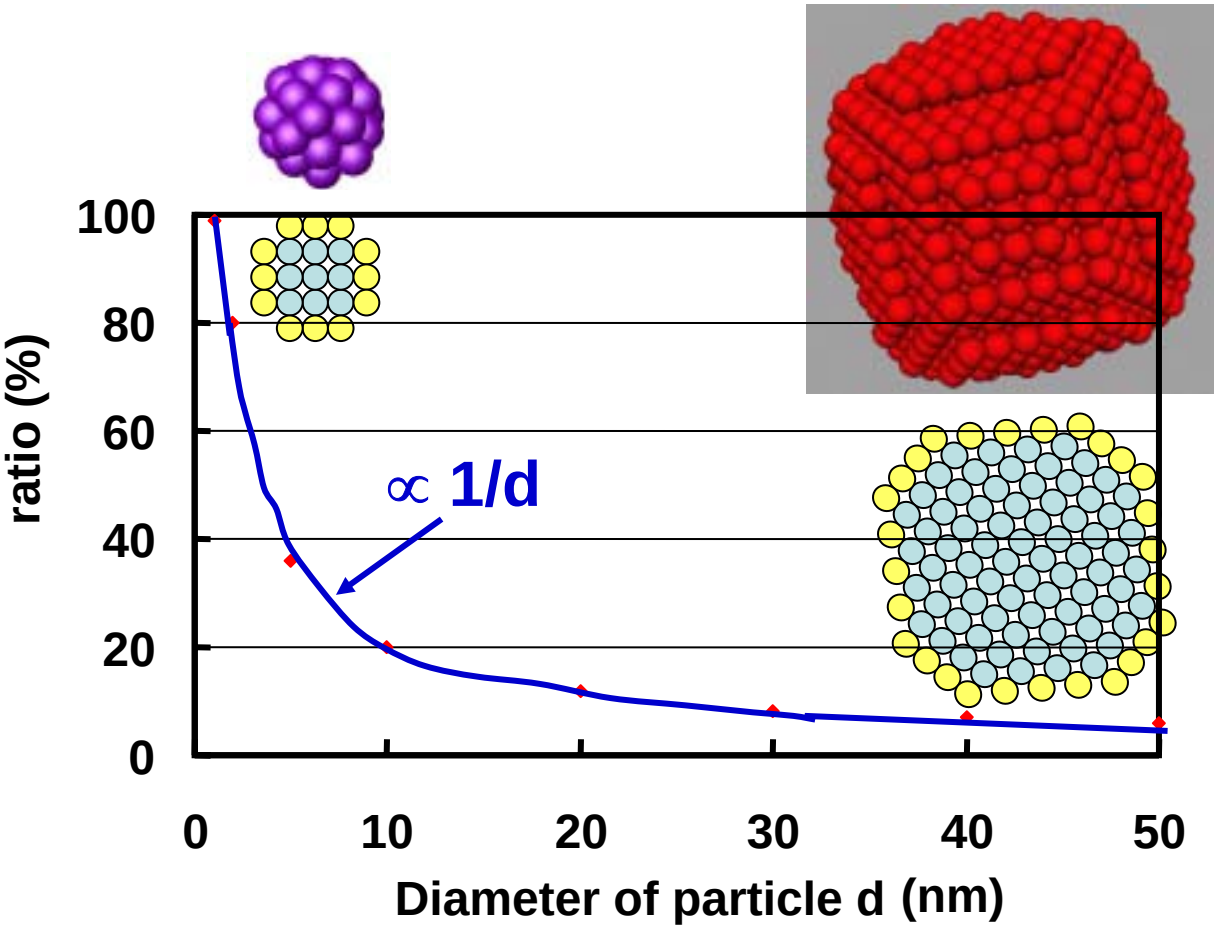

Enhanced catalytic effect

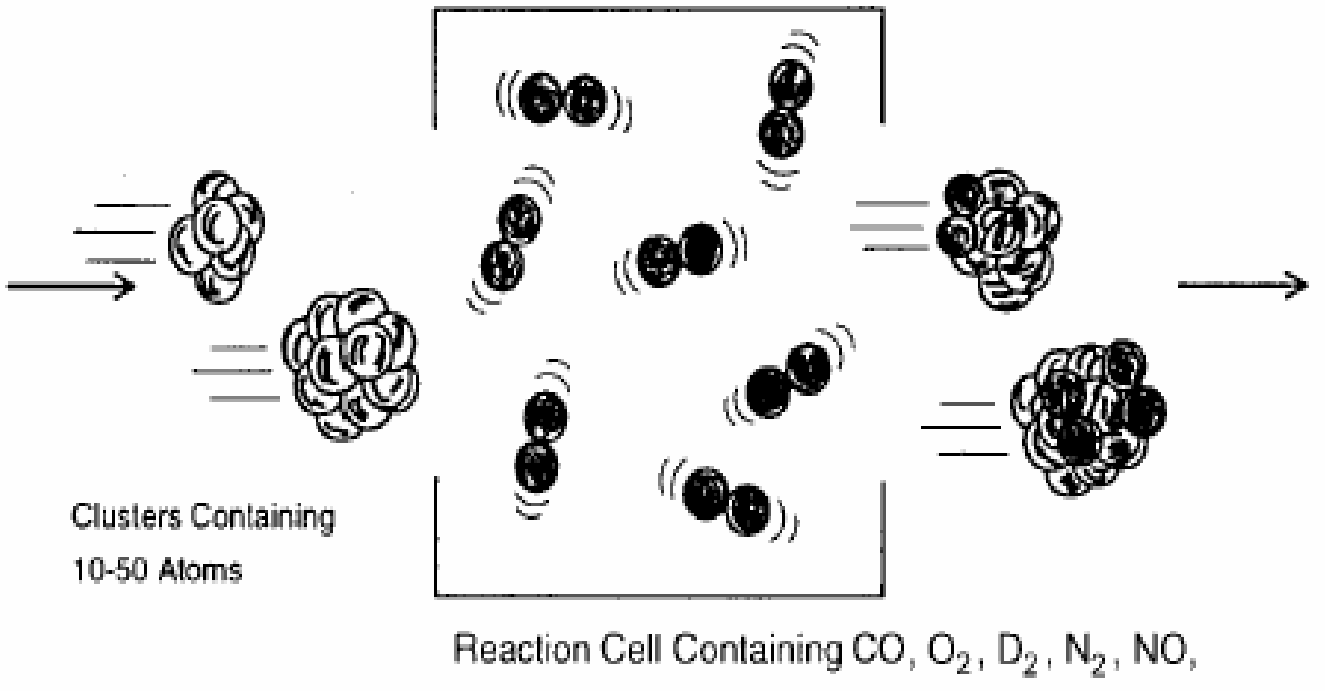

Au nanoparticle as an example

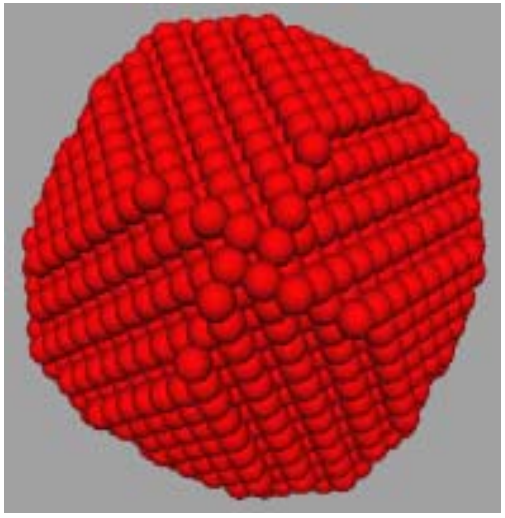

10 nm

$$E_F = (\hbar^2/2m)\,(3\pi^2 n)^{2/3}$$

$$g(E_F) = (3/2)\,(n/E_F)$$

$$\delta = 2/[g(E_F)V] = (4/3)\,(E_F/N)$$

Number of valence electrons (N) contained in the particles is roughly 40,000. Assume the Fermi energy (E_F) is about 7 eV for Au, then

$$\delta \sim 0.22 \text{ meV} \sim 2.5 \text{ K}$$

Electronic Structure of Single-wall Nanotubes

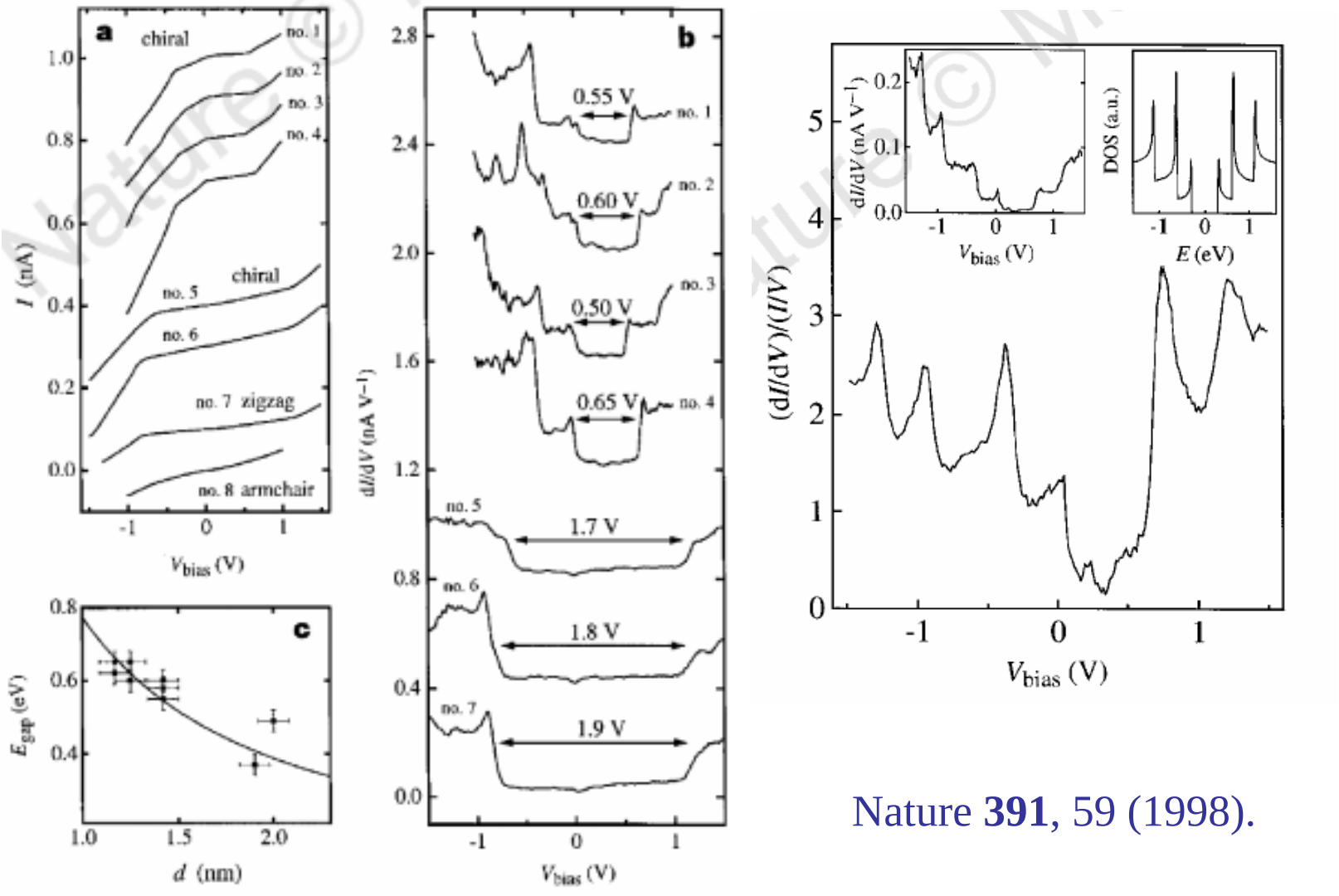

Nature **391**, 59 (1998).

Optical properties of nanoparticles (in the infrared range)

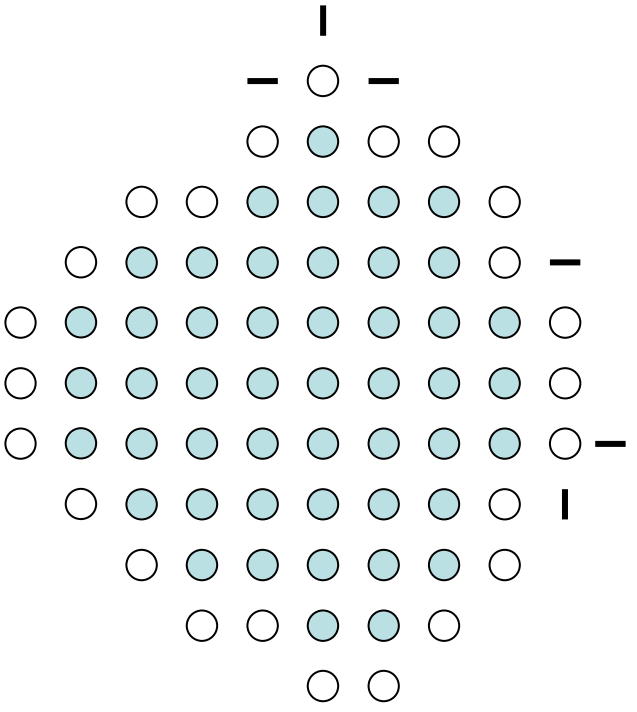

(1) Broad-band absorption:
Due mainly to the increased normal modes at the surface.

(2) Blue shift:
Due mainly to the bond shortening resulted from surface tension.

Optical properties of nanoparticles (in the visible light range)

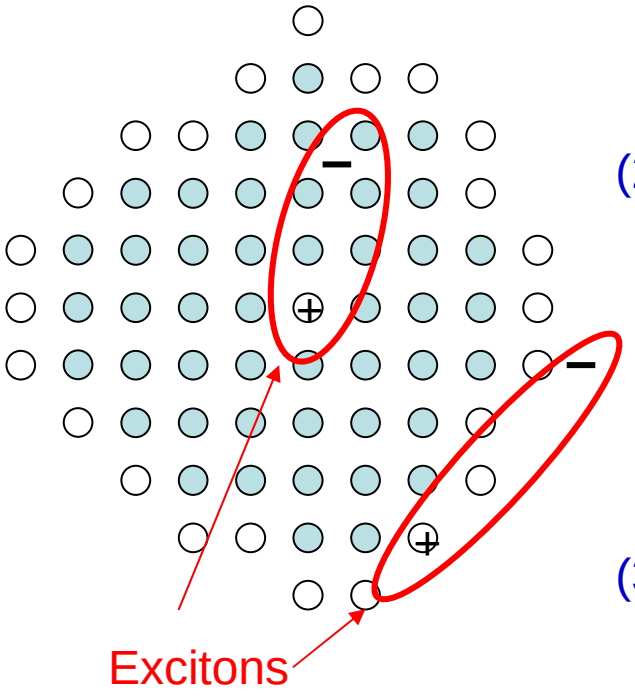

(1) Blue shift:

Due mainly to the energy-gap widening because of the size effect.

(2) Red shift:

Bond shortening resulted from surface tension causes more overlap between neighboring electron wavefunctions. Valence bands will be broadened and the gap becomes narrower.

(3) Enhanced exciton absorption:

Due mainly to the increased probability of exciton formation because of the confining effect.

Optical properties

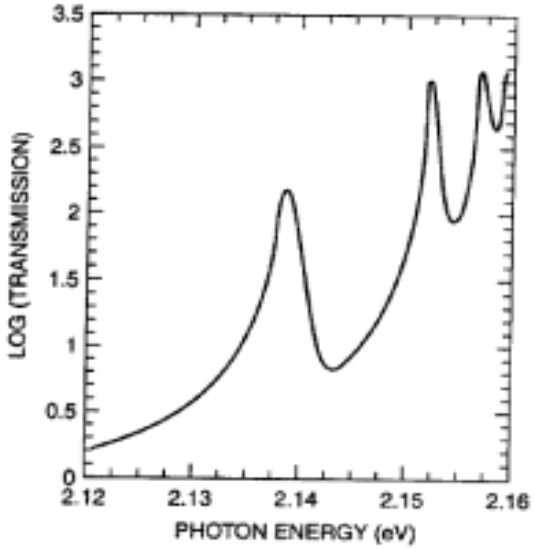

Figure 4.19. Optical absorption spectrum of hydrogen-like transitions of excitons in Cu_2O. [Adapted from P. W. Baumeister, *Phys. Rev.* **121**, 359 (1961).]

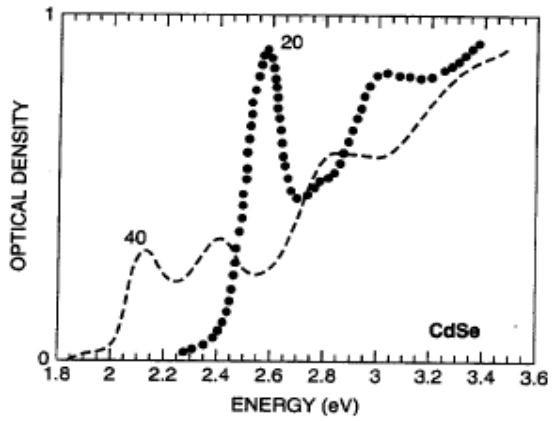

Figure 4.20. Optical absorption spectrum of CdSe for two nanoparticles having sizes 20 Å and 40 Å, respectively. [Adapted from D. M. Mittleman, *Phys. Rev.* **B49**, 14435 (1994).]

Semiconductor quantum dots

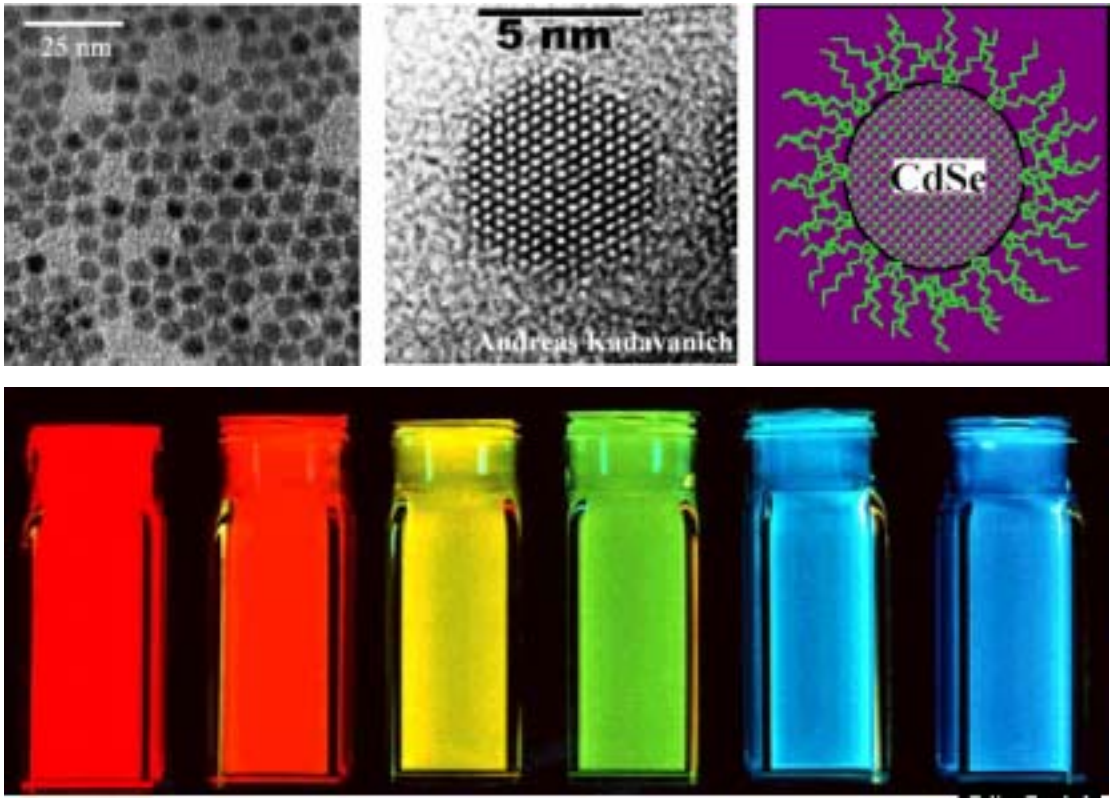

(Reproduced from Quantum Dot Co.)

Specific heat and magnetic susceptibility

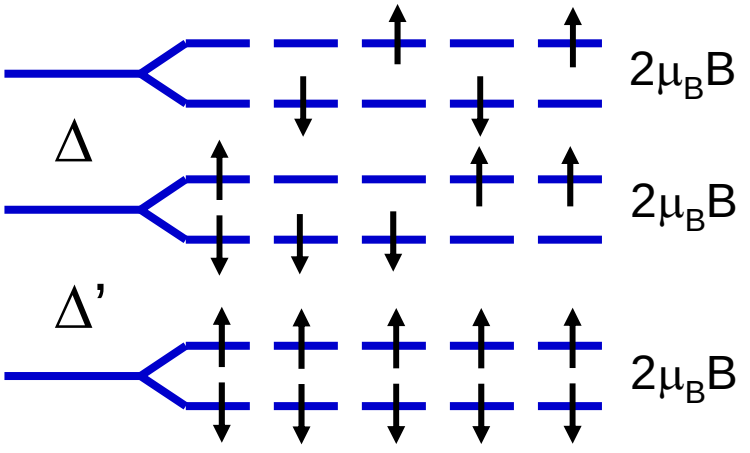

Even number of electrons

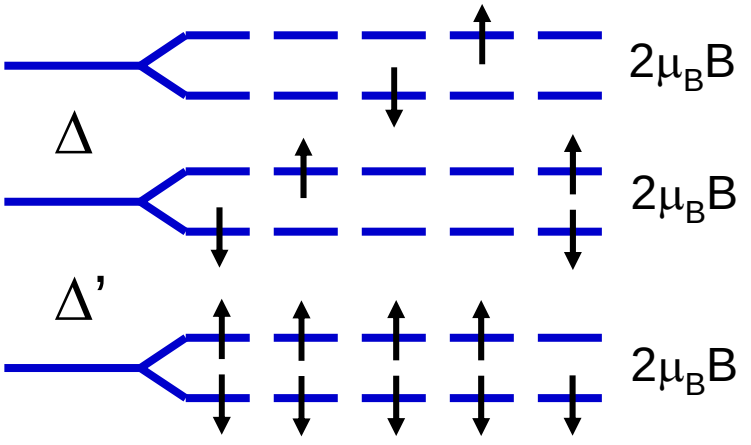

Odd number of electrons

$$Z_e \approx 1+2[1+\cosh(2\beta\mu_B B)\exp(-\beta\Delta)]+\exp(-2\beta\Delta)$$

$$Z_e \approx 2[\cosh(2\beta\mu_B B)][1+\exp(-\beta\Delta)+\exp(-\beta\Delta')]$$

$$C_e = 4k_B\beta^2\Delta^2\exp(-\beta\Delta)$$

$$\chi_e = 8\mu_0\mu_B^2\beta\exp(-\beta\Delta)$$

$$C_o = k_B\beta^2\Delta^2\exp(-\beta\Delta)$$

$$\chi_o = \mu_0\mu_B^2\beta$$

Varying structures of Ag clusters

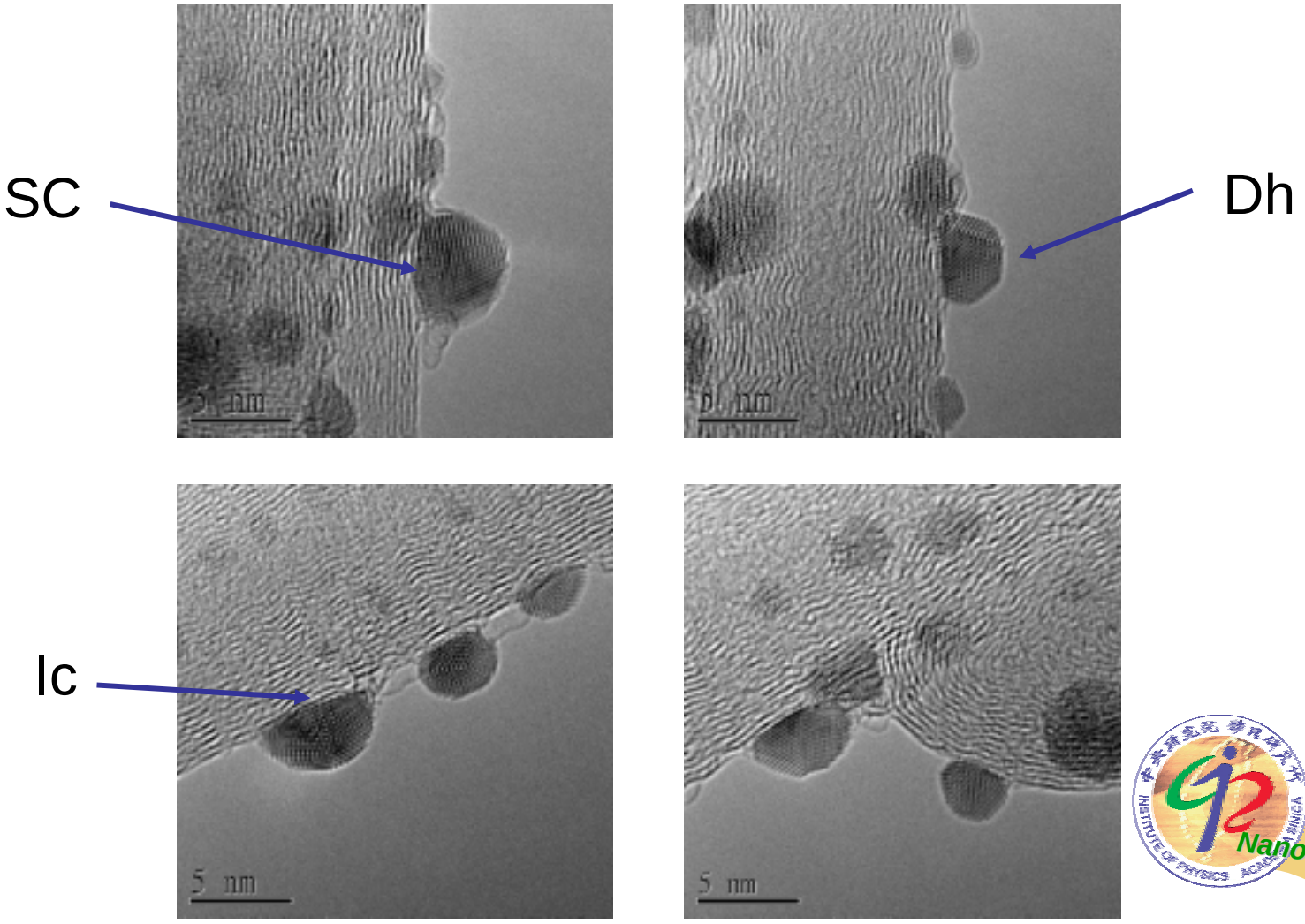

Atomic motion and recrystallization

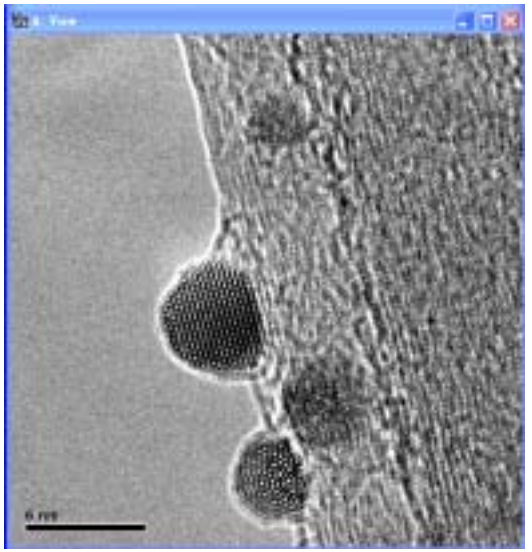

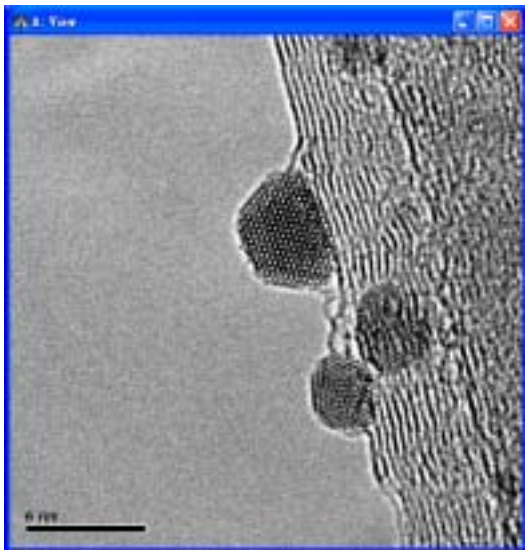

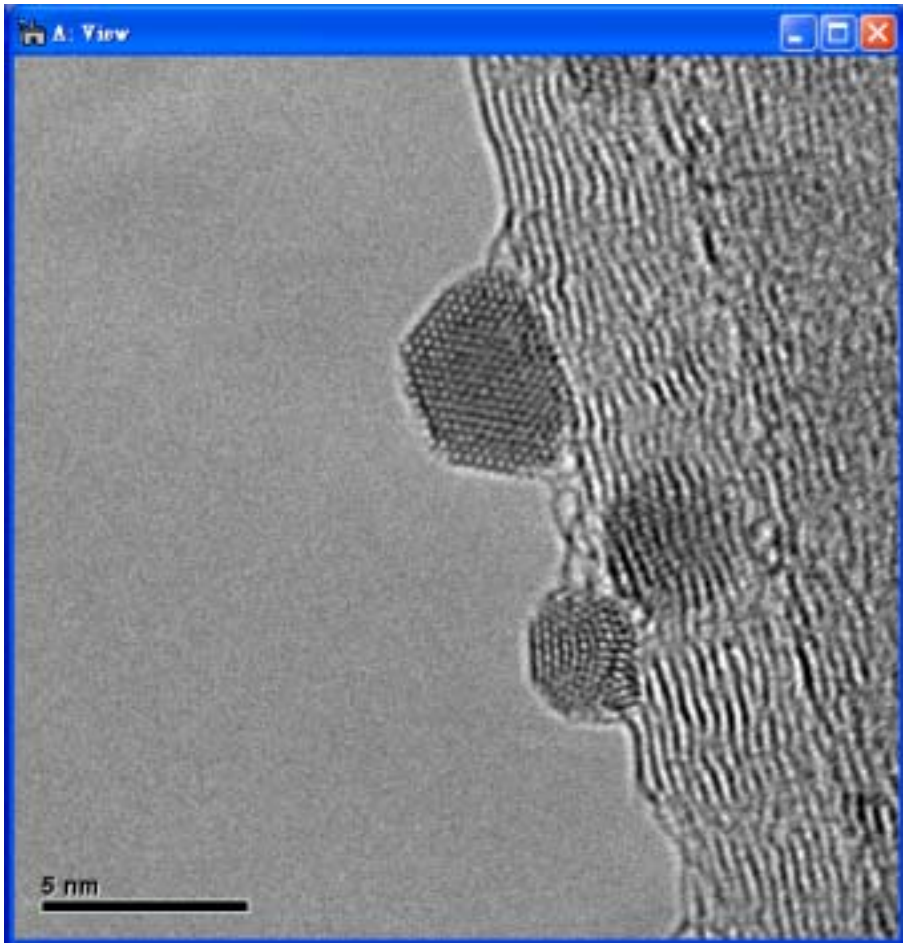

Room temperature

NanoSci Lab

Decahedra

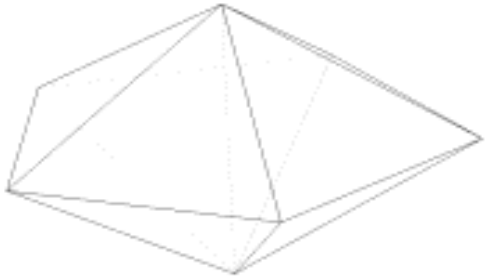

Classic

Ino’s

Marks’

Wulff construction

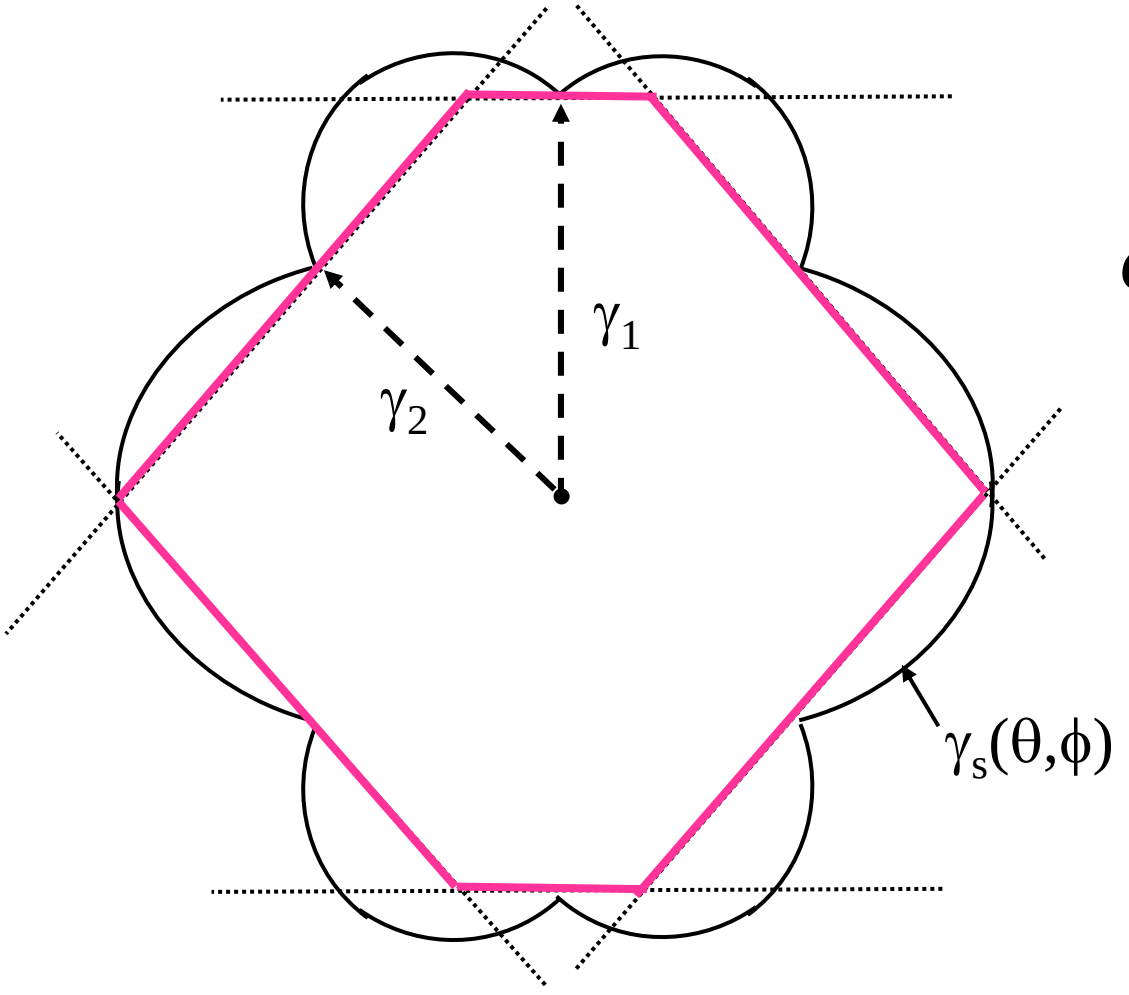

$$G = \int \gamma_s(\theta,\phi)\, dA$$

Single crystalline structures

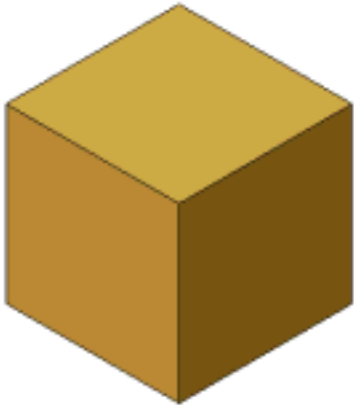

(a) cube

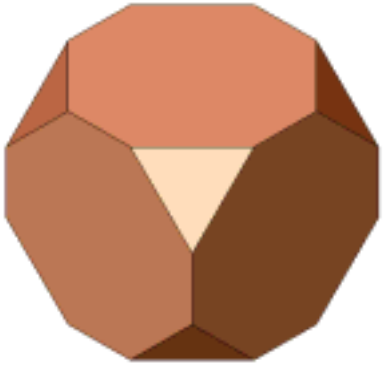

(b) truncated cube

(c) cuboctahedron

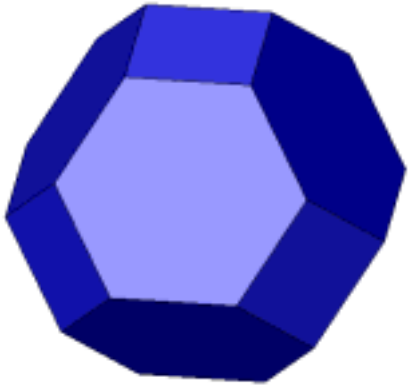

(d) truncated octahedron

(e) octahedron

NanoSciLab

Icosahedra

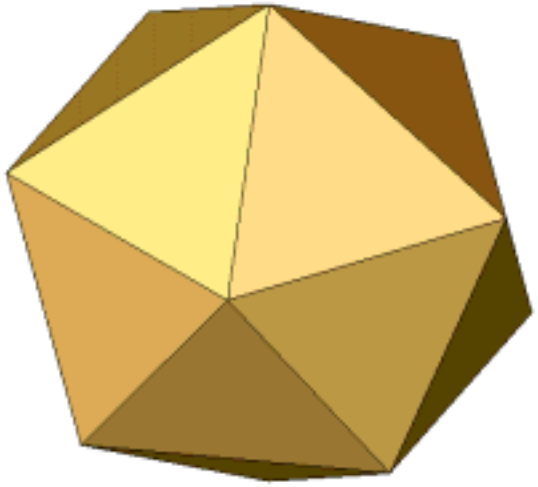

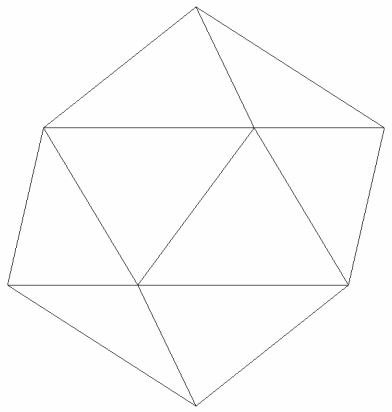

Size-dependent structures calculated for Ni clusters:

Icosahedra for 142 – 2300 atoms;

Marks' decahedra for 2300 – 17000 atoms;

Single crystal for > 17000 atoms.

C.L. Cleveland and Uzi Landman, J. Chem. Phys. 94, 7376 (1991).

Stability of crystalline phases

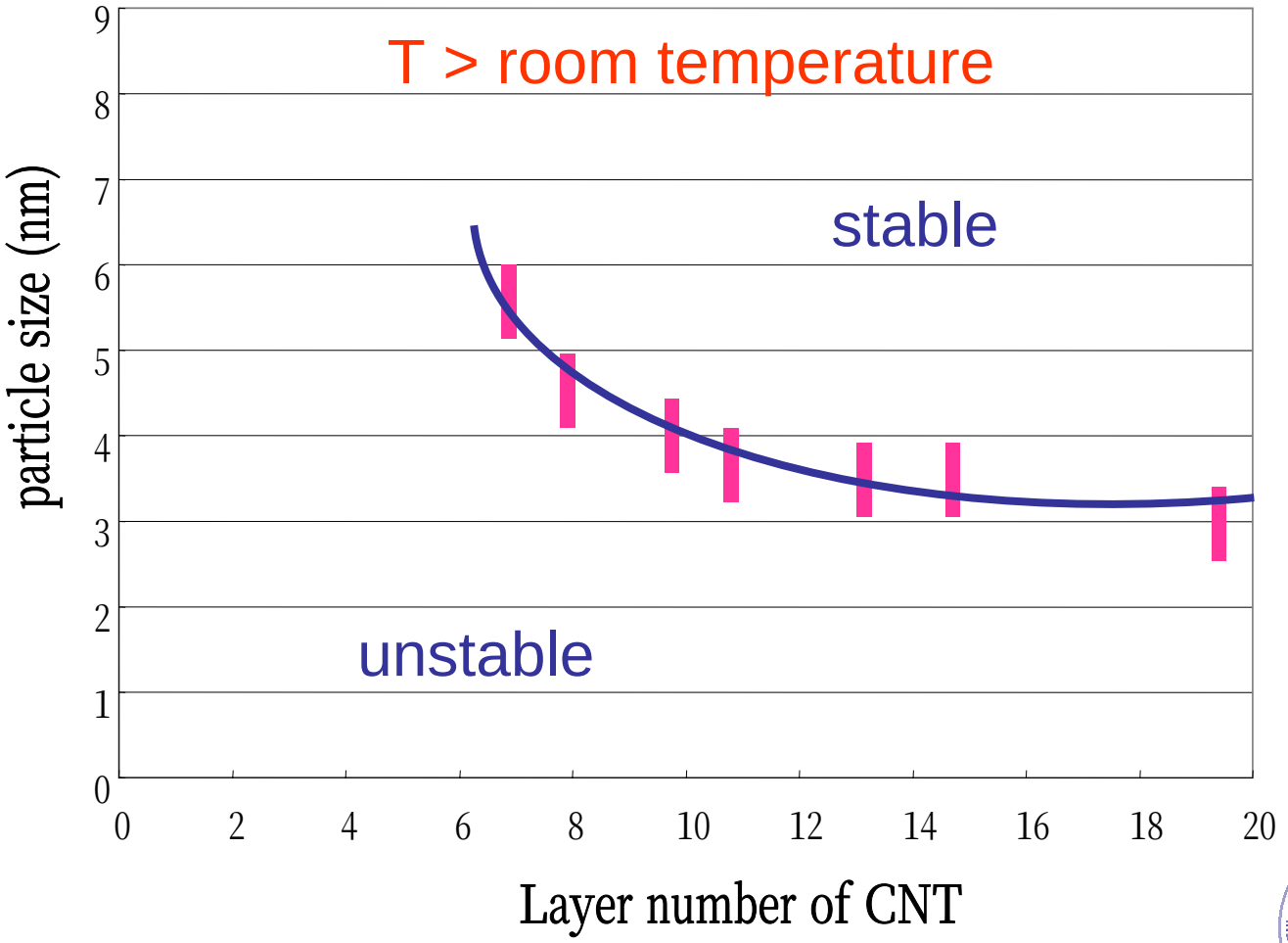

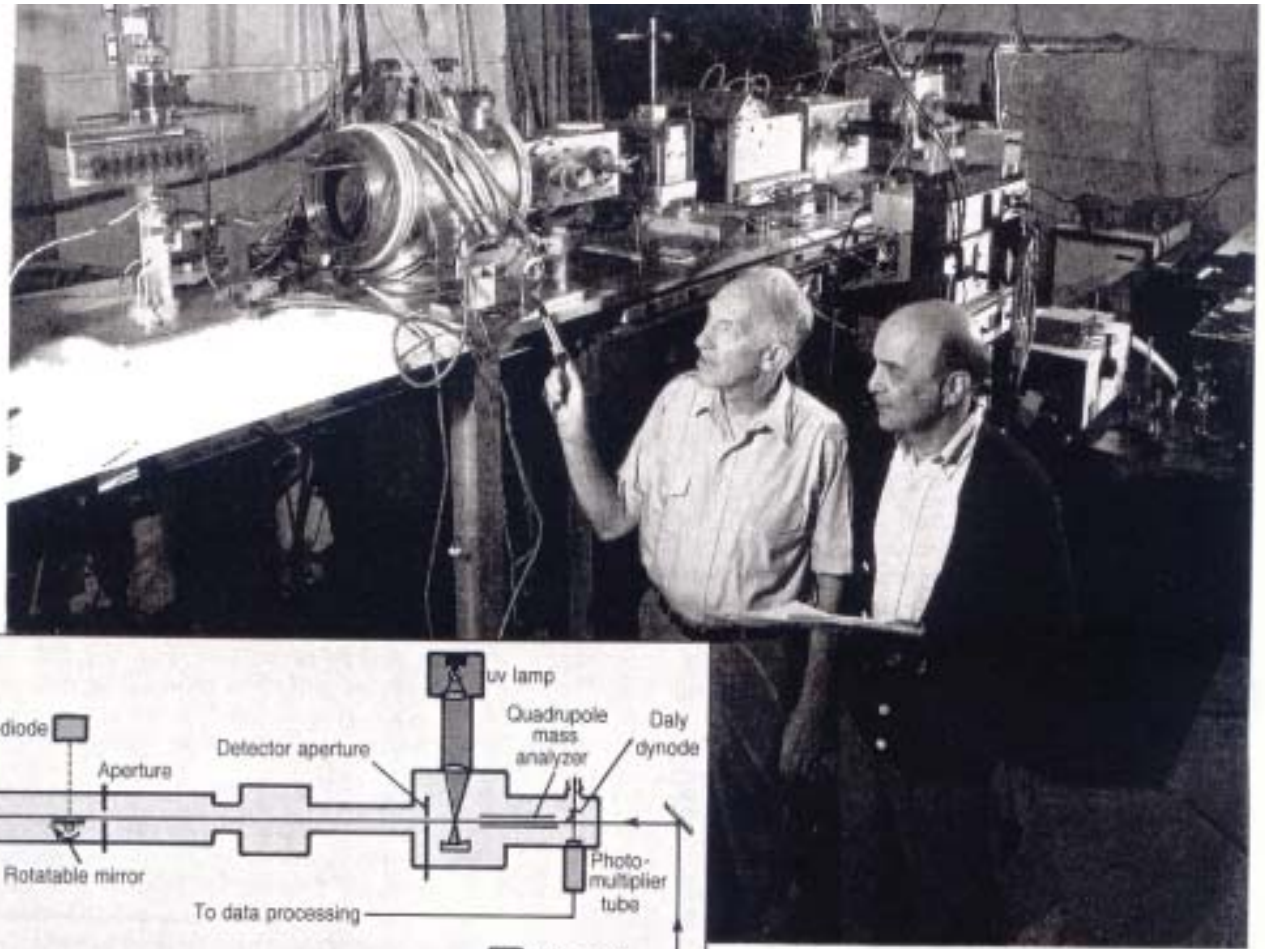

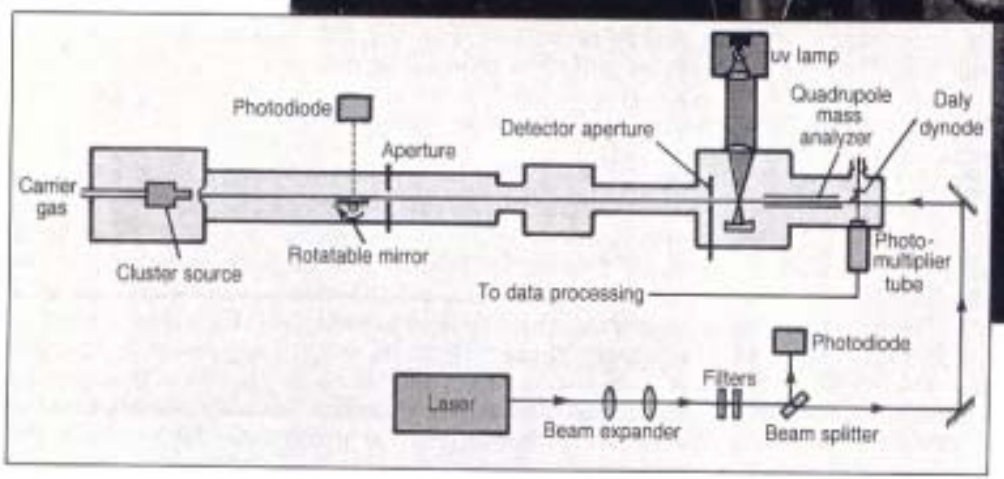
uv lamp
Photodiode
Quadrupole mass analyzer
Daly dynode
Detector aperture
Aperture
Carrier gas
Photo-multiplier tube
Rotatable mirror
Cluster source
To data processing
Photodiode
Filters
Laser
Beam expander
Beam splitter

Mass Analyzer

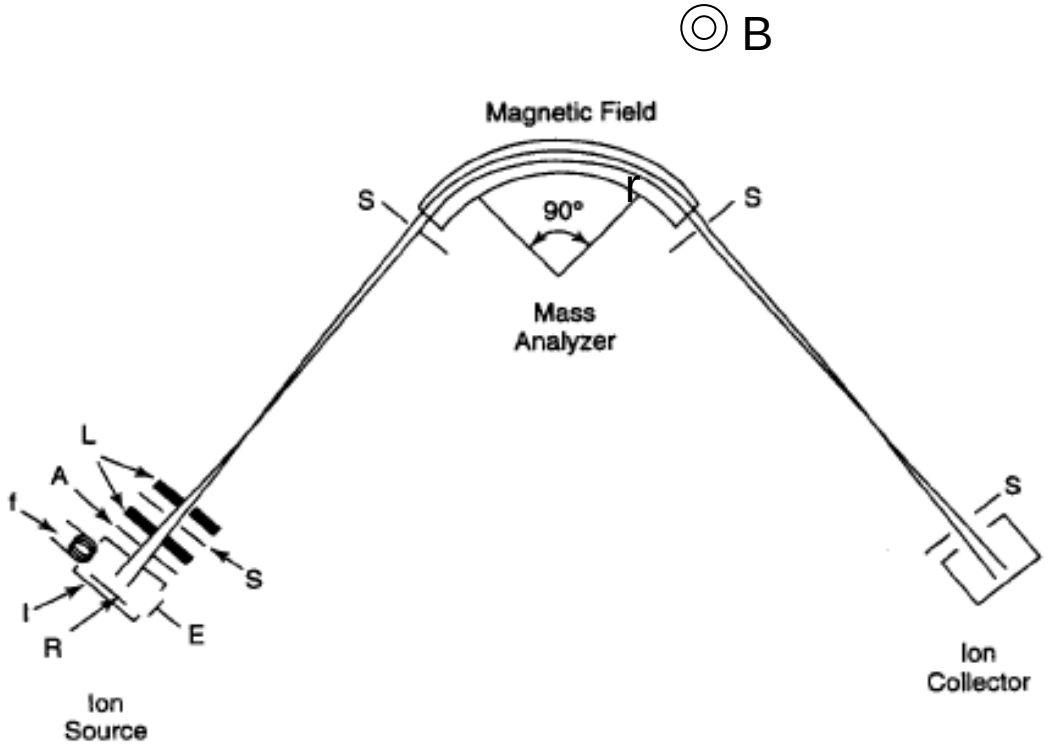

$qV = \frac{1}{2} mv^2$

$F = qvB = mv^2/r$

$m/q = \frac{1}{2} B^2r^2/V$

Figure 3.8. Sketch of a mass spectrometer utilizing a 90° magnetic field mass analyzer, showing details of the ion source: A—accelerator or extractor plate, E—electron trap, f—filament, I—ionization chamber, L—focusing lenses, R—repeller, S—slits. The magnetic field of the mass analyzer is perpendicular to the plane of the page.

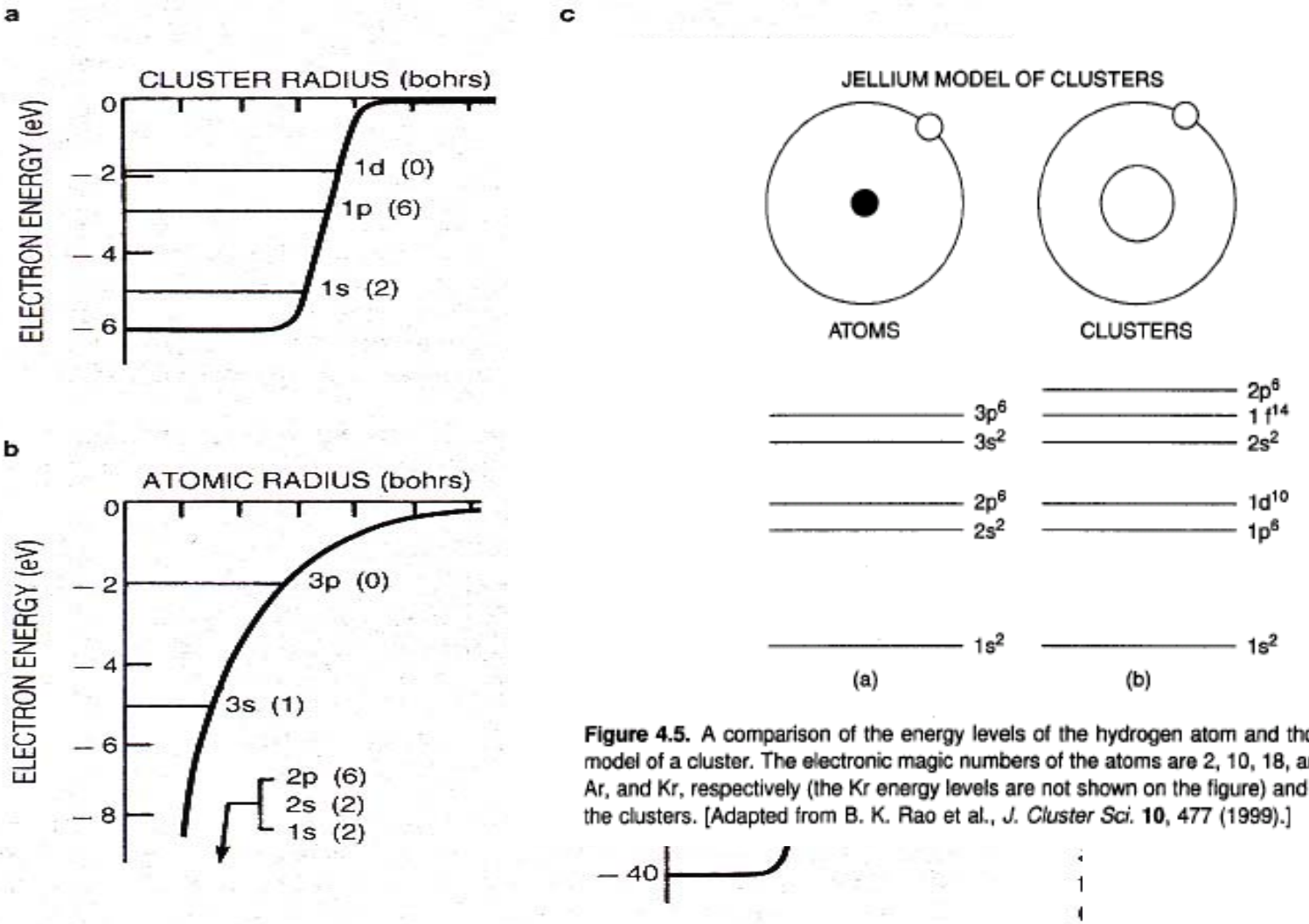

Figure 4.5. A comparison of the energy levels of the hydrogen atom and those of the jellium model of a cluster. The electronic magic numbers of the atoms are 2, 10, 18, and 36 for He, Ne, Ar, and Kr, respectively (the Kr energy levels are not shown on the figure) and 2, 18, and 40 for the clusters. [Adapted from B. K. Rao et al., *J. Cluster Sci.* **10**, 477 (1999).]

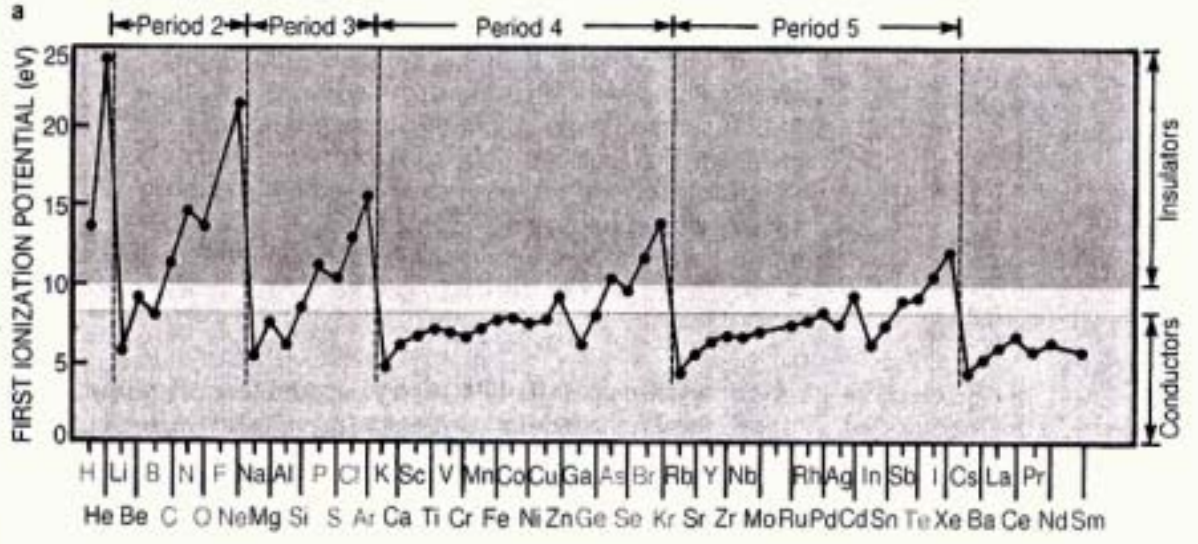

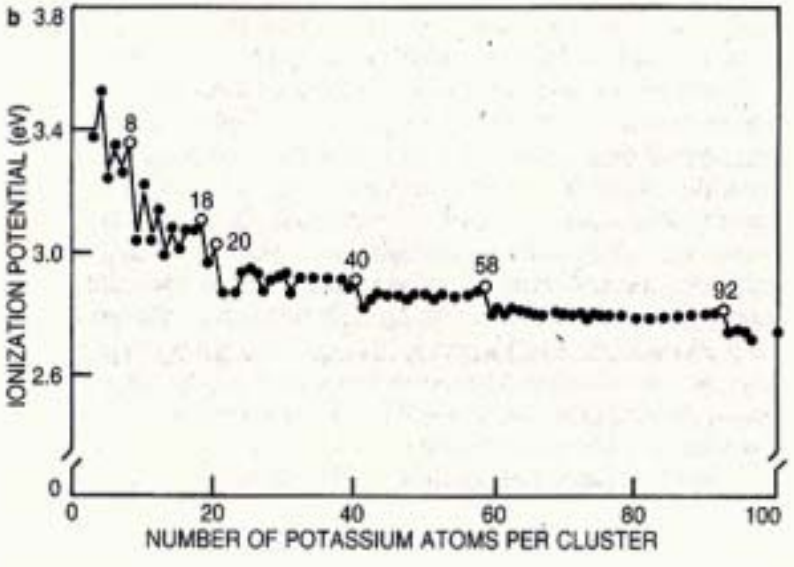

Shell structure: Two views. a: Atomic ionization potentials drop abruptly from above 10 eV following the shell closings for the noble gases (He, Ne, Ar and so on). For semiconductors (labeled in blue) the ionization potential is between 8 and 10 eV, while for conductors (red) it is less than 8 eV. It is clear that bulk properties follow from the natures of the corresponding atoms. (Adapted from A. Holden, *The Nature of Solids*, © Columbia U. P., New York, 1965. Reprinted by permission.) **b:** Ionization potentials for clusters of 3 to 100 potassium atoms show behavior analogous to that seen for atoms. The cluster ionization potential drops abruptly following spherical shell closings at $N = 8$, 20, 40 . . . . Features at $N = 26$ and 30 represent spheroidal subshell closings. The work function for bulk potassium metal is 2.4 eV. **Figure 3**

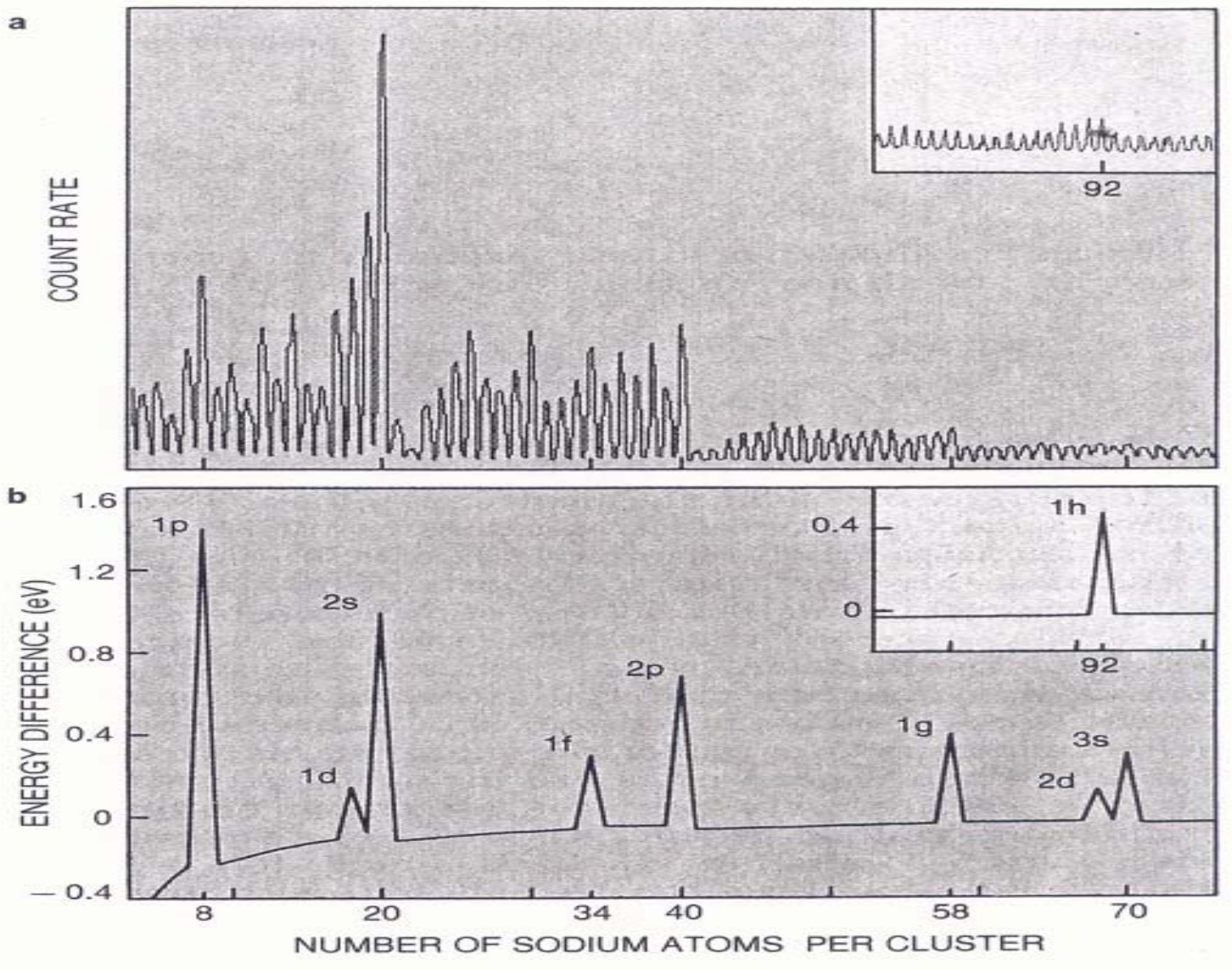
a
COUNT RATE
92
b
ENERGY DIFFERENCE (eV)
1.6
1.2
0.8
0.4
0
— 0.4
1p
2s
1d
2p
1f
1g
3s
2d
1h
0.4
0
92
8
20
34
40
58
70
NUMBER OF SODIUM ATOMS PER CLUSTER

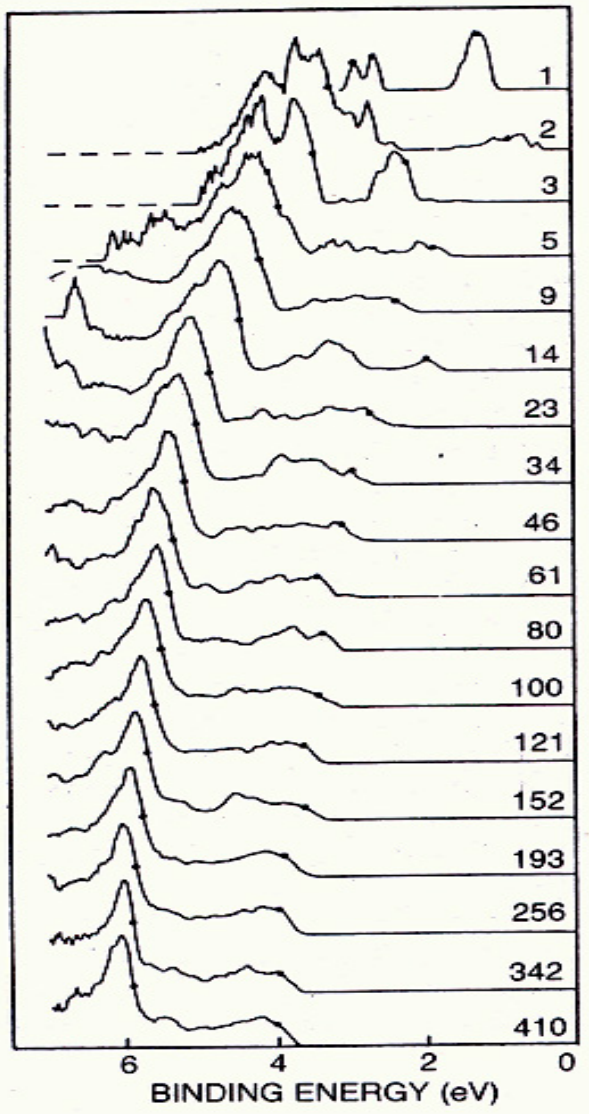

Ultraviolet photoemission spectra of ionized copper clusters Cu_N^- ranging in size from N of 1 to 410 show the energy distribution versus binding energy of photoemitted electrons. These photoemission patterns show the evolution of the 3d band of Cu as a function of cluster size. As the cluster size increases, the electron affinity approaches the value of the bulk metal work function. (Adapted from ref. 10.) **Figure 5**

Reactivity of nanoclusters

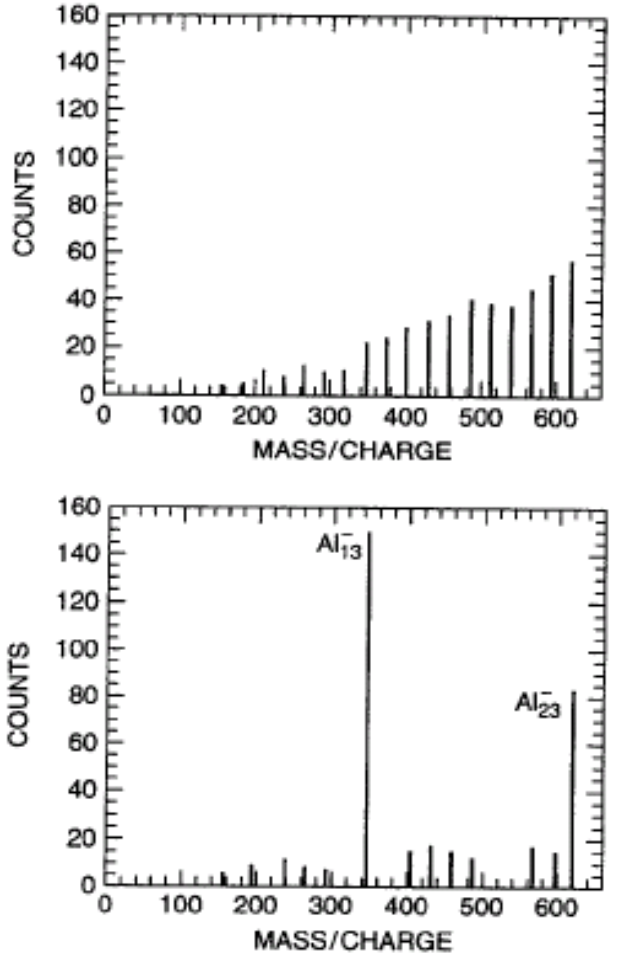

Figure 4.13. Mass spectrum of Al nanoparticles before (top) and after (bottom) exposure to oxygen gas. [Adapted from R. E. Leuchtner et al., *J. Chem. Phys.*, **91**, 2753 (1989).]

Magic clusters

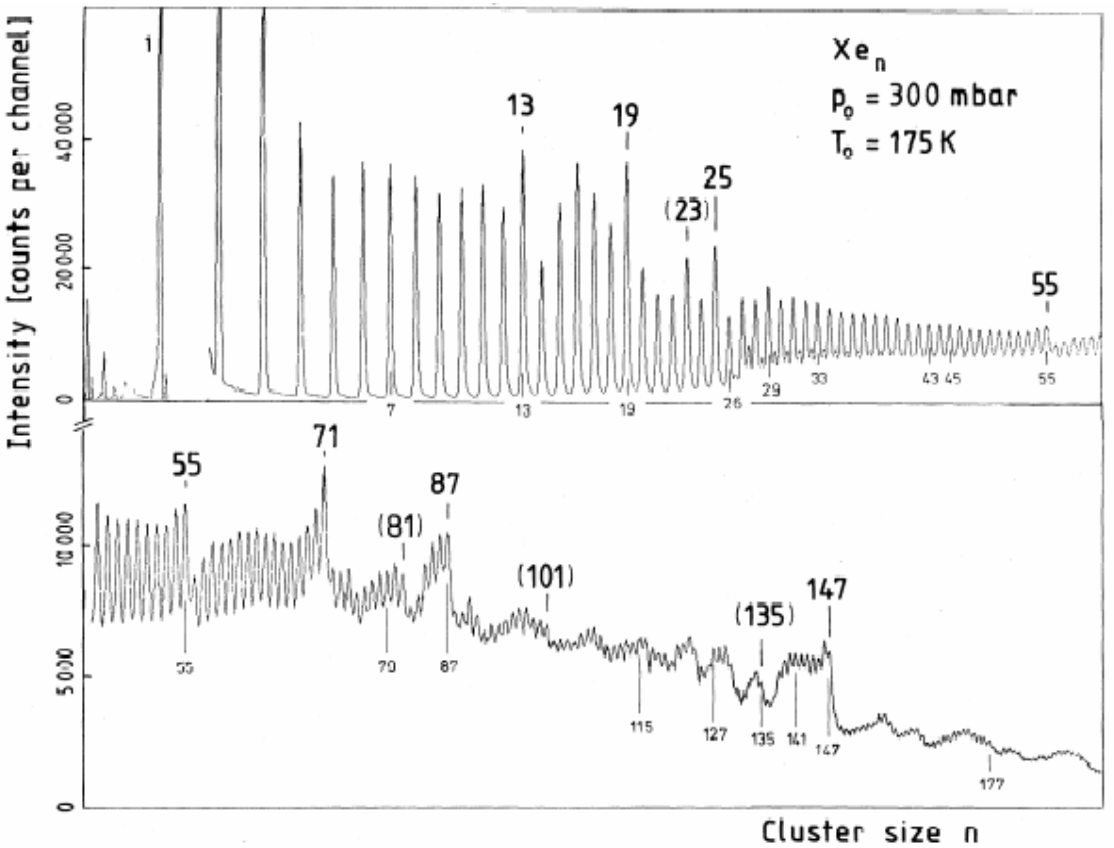

FIG. 1. Mass spectrum of xenon clusters. Observed magic numbers are marked in boldface; brackets are used for numbers with less pronounced effects. Numbers below the curve indicate predictions or distinguished sphere packings.

Mackay icosahedra

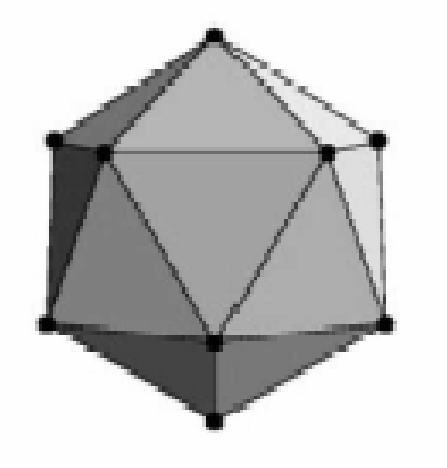

P = 1

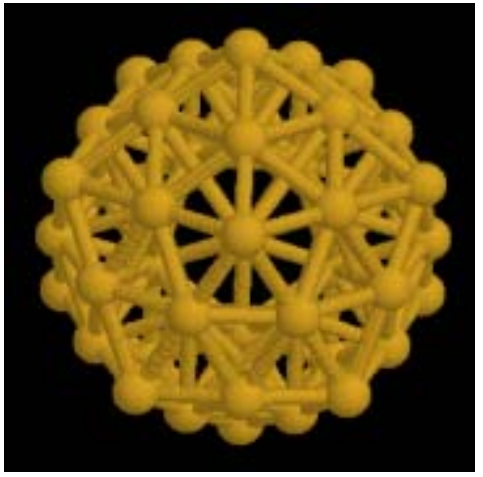

P = 2

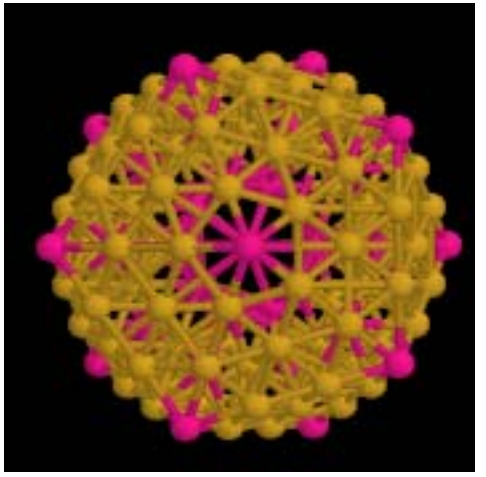

P = 3

20 fcc(111) faces

Shell model

$$N = 1 + \Sigma (10p^2 + 2)$$

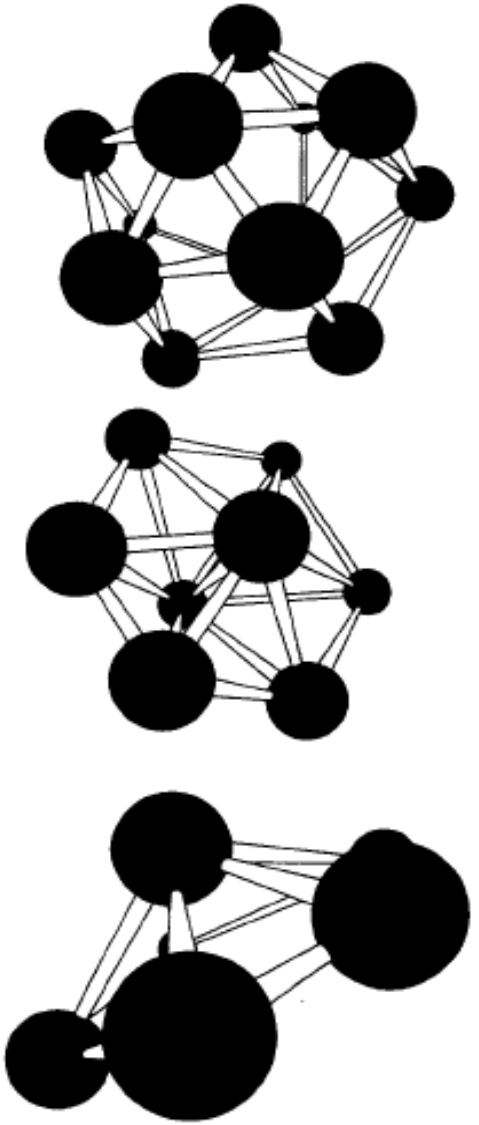

Icosahedra
(13)

Decahedra
(8)

Pentagonal pyramid
(6)

Figure 4.8. Illustration of some calculated structures of small boron nanoparticles. (F. J. Owens, unpublished.)

Fullerenes

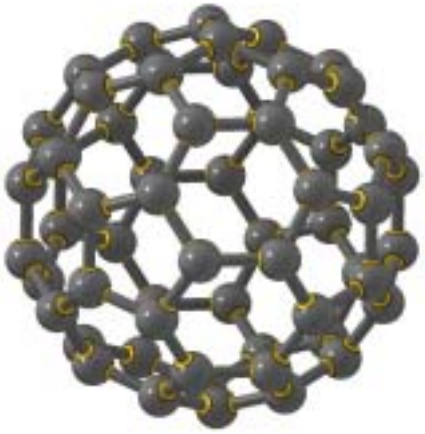

C_{60}

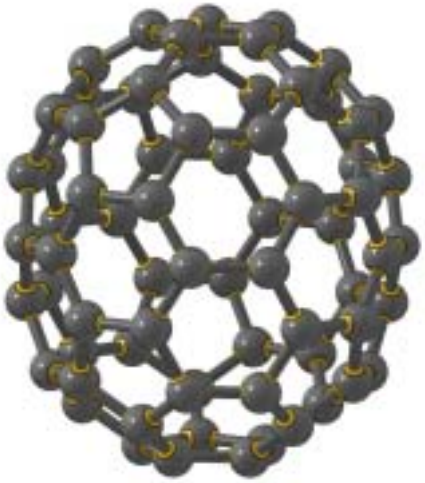

C_{70}

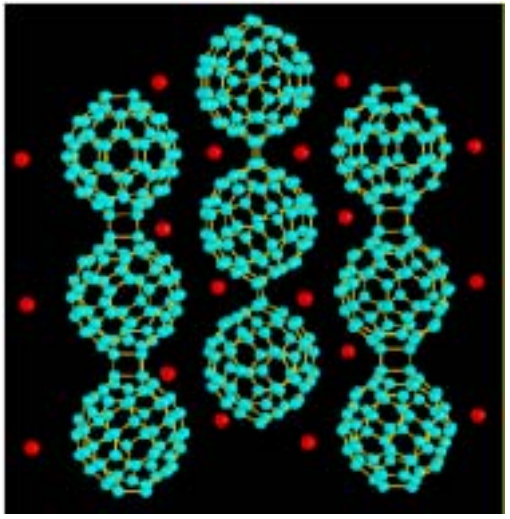

Rb_3C_{60}

$T_c = 29\ K$

Quantum corral

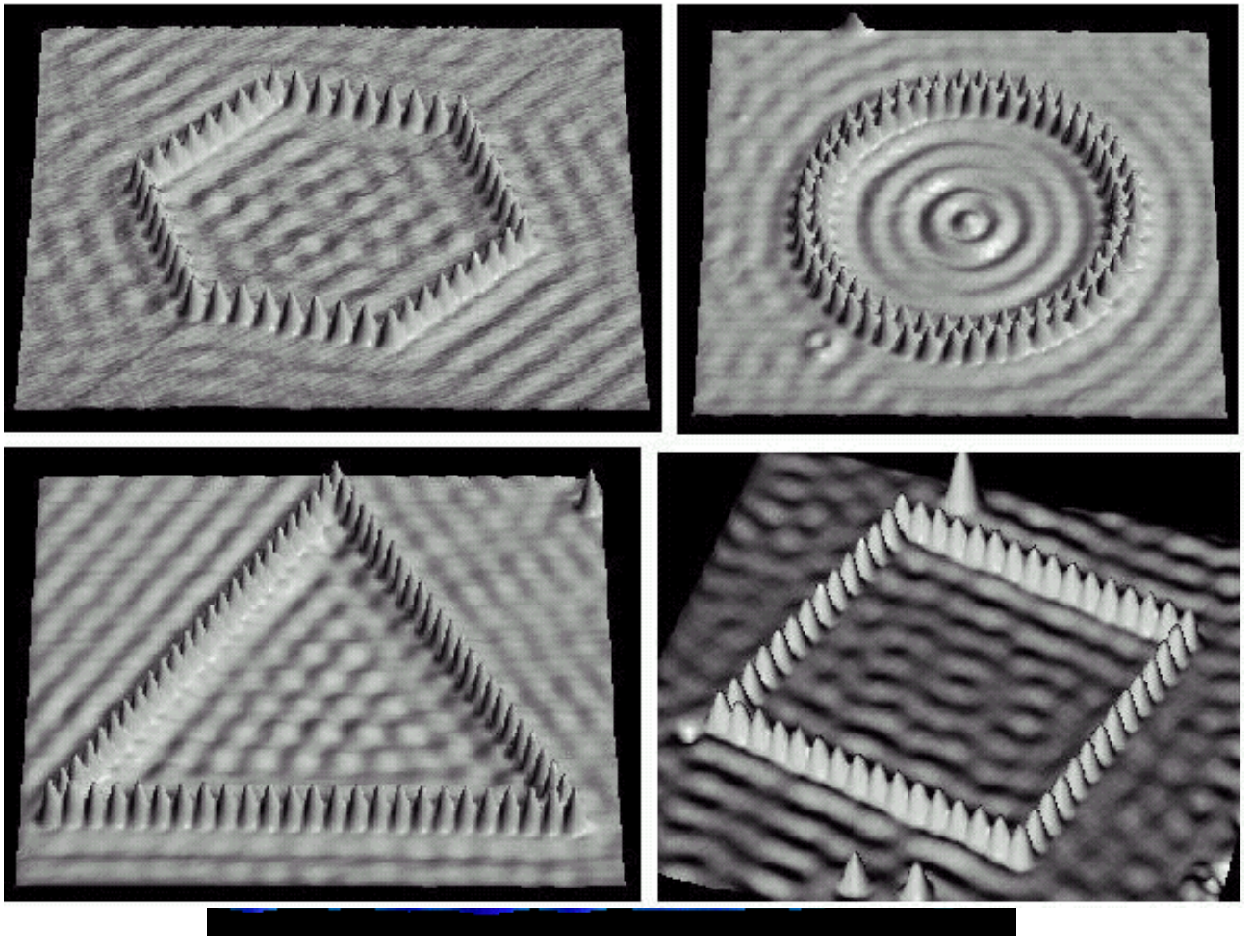

D.M. Eigler, IBM, Amaden

Artificial atom